Data-driven weathering layer statics for hardrock imaging: Solutions based on first-breaks and surface waves

CONFERENCE & EXHIBITION
NEAR SURFACE GEOSCIENCE'20

EAGE

Data-Driven Weathering Layer Statics for Hardrock Imaging: Solutions Based on First-Breaks and Surface Waves

B. Brodic[1], M. Papadopoulo[2], L. Bräunig[3], V. Socco[2], D. Draganov[4], S. Buske[3], A. Malehmir[1]

[1] Uppsala University; [2] Politecnico di Torino; [3] TU Bergakademie Freiberg; [4] Delft University of Technology

Summary

Seismic methods are routinely used for hardrock imaging and mineral-exploration purposes. However, hardrock seismic data requires careful processing, where weathering layer - refraction static corrections have shown to be of great importance for successful imaging. In our study, six differently obtained data-driven weathering layer static solutions are analyzed and compared using a seismic dataset from a mining site in Sweden. Three of the six approaches utilize first-breaks and are based on (1) the standard refraction-inversion method (RI), (2) the application of the RI after adding additional first-breaks via supervirtual seismic interferometry (SVSI), and (3) a tomography-based static solution (Tomostatics). The other three approaches employ surface-waves and are based on (4) the direct transformation of SW dispersion curves, (5) joint inversion of dispersion curves as well as first-breaks and (6) surface-wave tomography. All tested methods were successful in enhancing coherency of the main ore body reflection. A crosscutting reflection can also be seen following the first-break based refraction statics, with highest coherency seen after the application of the SVSI-enhanced RI refraction statics. The examples presented suggest that these methods can be complementary and in the absence of notable first-breaks, surface waves can be utilized to estimate weathering layer static corrections.

Introduction

Crystalline (hardrock or igneous) settings host a substantial fraction of planet's mineral wealth in terms of metals such as copper, nickel, lead, zinc, gold, iron and their associated rare-earth elements. Irrespective of dealing with brown- or greenfield exploration in such terrains, among other geophysical methods, the seismic method has become a standard tool for high-resolution and high-quality imaging of mineralized structures as well as for direct targeting (Malehmir et al., 2019). However, seismic exploration in hardrock environments is not an easy task due to their heterogeneous nature often causing strong signal scattering and diffractions, weak target reflectivity and complex 3D structure of the deposit. The presence of an inhomogeneous and strongly weathered overburden adds further complications. All these factors contribute to lowering the signal-to-noise (S/N) ratio of seismic datasets, making the seismic imaging work challenging. Therefore, hardrock seismic imaging requires tailored processing strategies, where for example, refraction static - weathering layer corrections have shown to be of great importance for successful imaging (Eaton et al., 2003). In our study, we evaluate six independently obtained, data-driven weathering layer static solutions.

Three of the six approaches utilize first-breaks, hence fall under the refraction statics category, namely:

1. Refraction-inversion (RI) based static solution (Woodward, 1992) implemented in commercial processing software;
2. Improvement of RI by adding additional first-breaks using cross-correlation-based supervirtual seismic interferometry (SVSI; Alshuhail et al., 2012; Place and Malehmir, 2016);
3. Independently obtained (Bräunig et al., 2020) tomography-based static solution (Tomostatics; Zhang and Toksöz, 1998).

The remaining three employ surface-waves (SW) to obtain near surface velocity from which weathering layer static corrections can be directly computed (Papadopoulou et al., 2020):

4. Direct statics estimation from SW dispersion curves (DCs) with the Wavelength-Depth (W/D) method (Socco et al., 2017; Socco and Comina, 2017)
5. Joint inversion of SW DCs and first-breaks (Boiero and Socco, 2014);
6. SW tomography (Boiero 2009).

All weathering layer static corrections were applied on a 2D seismic dataset acquired at a mining site in central Sweden (Figure 1).

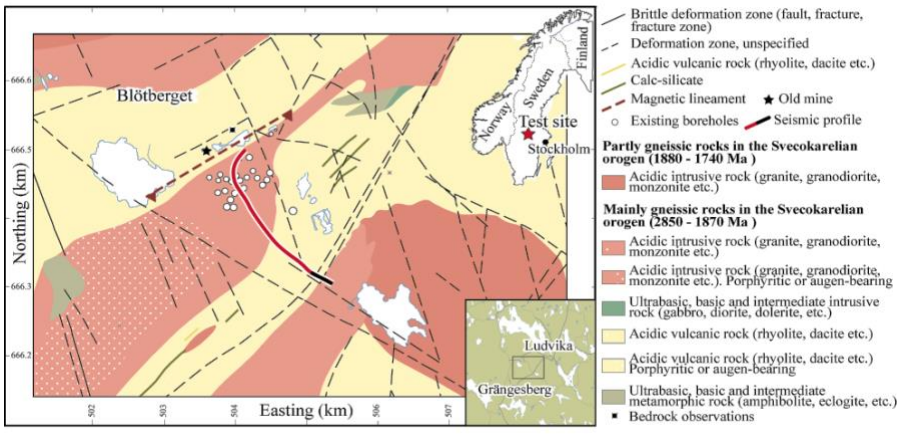

Figure 1 *Location of the Blötberget site and the 2D seismic profile with the main geologic and tectonic features. Red and black portions of the seismic profile correspond to cabled and wireless receiver parts of the profile, respectively. Figure modified from Markovic et al. (2020).*

Data acquisition and site

The seismic data used to test the different weathering layer static corrections were acquired in October 2016 at the Blötberget iron-oxide mining site of the Bergslagen mineral province in central Sweden (Figure 1). Mining in Bergslagen goes back to the 16th century, and the entire region is well known for its high-quality iron-oxide ores. However, the downturn of iron ore prices during the 1970's resulted in the closure of several mines in the region, including Blötberget. With the technological advancements and favorable market conditions nowadays, mining is planned to resume at Blötberget in the near future,

imposing the need for reevaluation of the mineral resource potential. The skarn-type iron-oxide or apatite-rich iron-oxide deposits are hosted within Paleoproterozoic age (1.9–1.8 Ga) metamorphosed volcano-sedimentary rocks (Figure 1). At Blötberget, the deposits occur in magnetite and hematite-rich sheet-like horizons (up to 30-50 m thick) dipping towards southeast down to at least 800 m, based on the *a-priori* borehole information and earlier geophysical studies (Malehmir et al., 2017). Data acquisition involved 427 cabled vertical 10-Hz geophones spaced at 5 m (red portion of the seismic profile in Figure 1) and 24 single-component wireless recorders with geophones of the same type spaced at 10 m (black portion in Figure 1). A 500 kg vertical drop-hammer seismic source was used with 387 source points collocated with all accessible receiver locations. Details of the acquisition and results can be found in Markovic et al. (2020).

Methods for weathering layer static solution

A standard approach for calculating weathering layer - refraction statics corrections is based on picking first-breaks on all seismic traces. The first-breaks are then used to obtain a velocity model of the near surface beneath every source or receiver position. Layered-based RI or commonly known as generalized linear inversion (GLI) as well as Tomostatic methods are often used for this purpose. In both cases, the velocity model is perturbed until the difference between picked and modelled first-break traveltimes is minimized in a least-square sense (Woodward, 1992; Zhang and Toksöz, 1998).

Both the RI and the Tomostatics solutions are first-break dependant, but the S/N ratio of the seismic dataset can be variable making the first-break picking challenging, particularly at far-offsets. To enhance the coherency of the low S/N-ratio events, SVSI was proposed (Alshuhail et al., 2012; Place and Malehmir, 2016 and references therein). The SVSI can be used to retrieve different seismic events, and its application to the refracted arrivals of a receiver pair yields a seismic trace with supervirtual-refraction traveltimes. The S/N ratio of the supervirtual trace is enhanced by the square root of the number of sources that contribute to the particular receiver pair. SVSI is most commonly applied by cross-correlation, cross-coherence or deconvolution of receiver pairs. Here we have applied SVSI using cross-correlation. Figure 2 shows an exemplary shot gather with all events muted except the first-break window, before and after application of the SVSI. Both the amplitudes and coherency of the refracted arrivals are significantly enhanced following SVSI. After applying SVSI, the number of picked traveltimes has increased by approximately 13% (raw data - 135523 picks, after SVSI - 153593 picks). The re-picked first-breaks are used for another iteration of the RI statics.

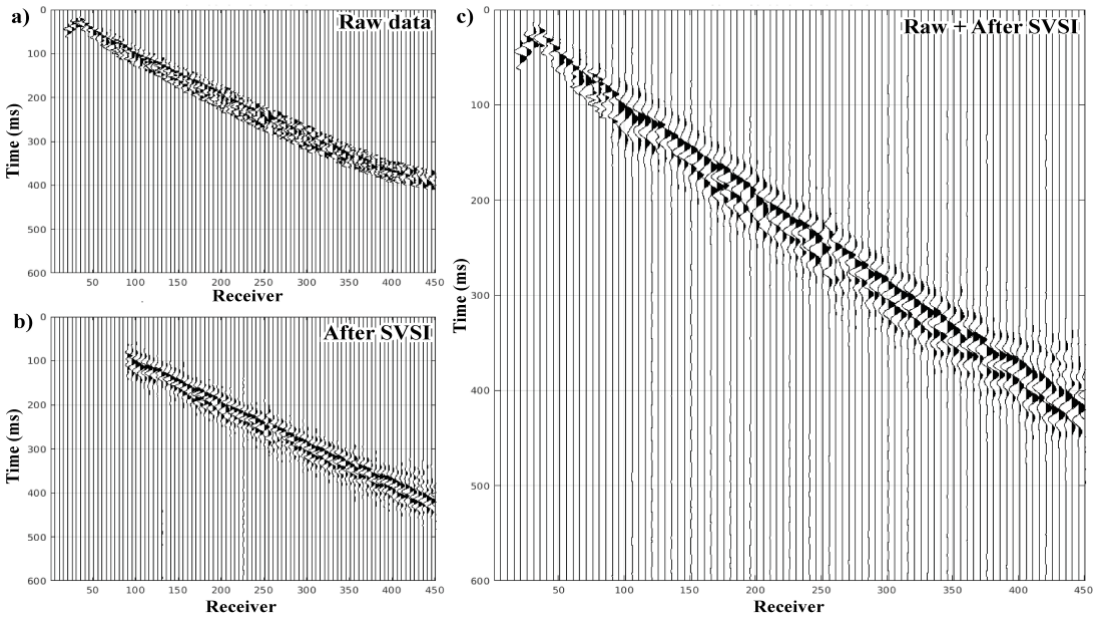

Figure 2 *First-breaks of an exemplary shot gather (a) before and (b) after application of the cross-correlation based SVSI algorithm. (c) The result after trace-by-trace stacking of the raw and the SVSI-enhanced data. Both amplitude strength and coherency are clearly improved.*

Regarding the SW-based solutions, the first approach (SW DC-W/D) provided the static time shift directly from the SW dispersion curves (DCs), without any a priori information. It is the fastest of all SW-based solutions, since it requires the inversion of only one DC and the subsequent direct transformation of the entire set of DCs into a time-average V_S and a time-average V_P model. The second approach (SW-BW), provided a V_P model (and the corresponding static shifts) inverting jointly the SW DCs and the first-breaks with the code of Boiero and Socco (2014). The third solution (SW Tomography statics) was retrieved by combining SW tomography, a method based on the tomographic V_S inversion of the dispersion curves between pairs of receivers, and the W/D method. This method also does not require any a priori information and, even though more computationally expensive due to the large number of required path-average DCs, exhibits higher lateral and vertical resolution.

Seismic stacked sections and comparison of results

Figure 3 shows a comparison of a reflection stacked section (Fig. 3a) without static correction and after application of the six different static solutions (Fig. 3b-g). All stacked sections have been processed using a conventional processing scheme consisting of CDP binning (2.5 m), refraction - weathering layer statics (long-wavelength only), AGC (250 ms), bandpass filtering (40-50-110-130 Hz), NMO correction (constant 6500 m/s), AGC (200 ms), stack, bandpass filtering (40-60-100-120 Hz), *f-x* deconvolution, amplitude balancing. Due to the significant crookedness of the profile line, SW-based statics are limited to the only a portion of the profile, as marked in Figure 3 with corresponding CDP numbers and the dashed lines. We can note that all six static solutions enhance successfully the main reflection, but the RI solution after SVSI also results in the highest coherency of the crosscutting event.

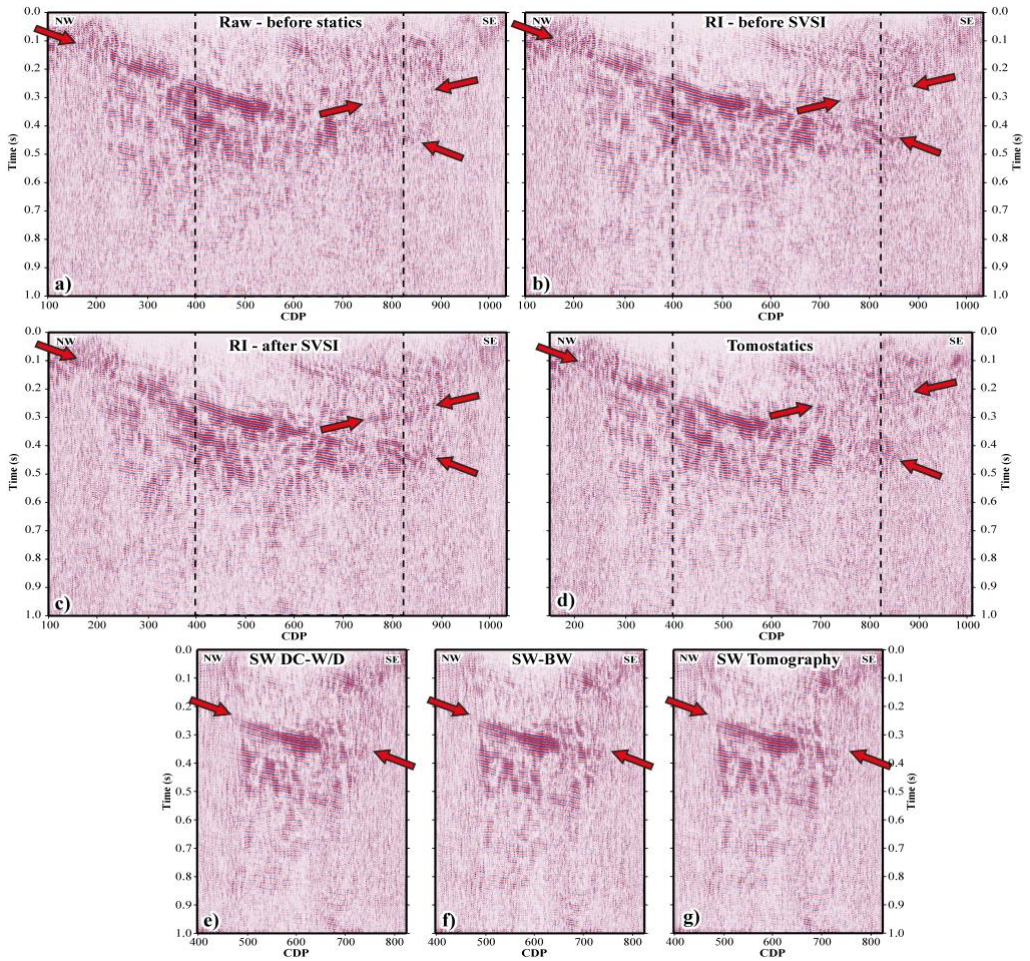

Figure 3 *Comparison of unmigrated stacked sections before and after application of different static solutions (40 m reference depth): (a) no statics, (b) RI statics, (c) RI after SVSI statics, (d) Tomostatics, (e) SW DC-W/D statics, (f) SW-BW statics and (g) SW Tomography statics. Arrows point at the main mineralization (SE dipping) and the crosscutting reflection (NW dipping).*

Conclusions

Six differently obtained data-driven weathering layer static solutions, three first-break based and three surface-wave (SW) based, were compared using a hardrock seismic dataset acquired in central Sweden. The tested methods were successful in enhancing the coherency of the main ore-body reflection; a crosscutting reflection is only partly enhanced after Tomostatics, further enhanced after Refraction-Inversion-based refraction statics but clearly enhanced after application of supervirtual seismic interferometry to provide more first-breaks and improve the Refraction-Inversion solution. All three SW-based methods had a similar performance in imaging the main reflector, with statics derived using SW tomography providing the highest quality, due to the high resolution achievable with SW tomography. The performance on enhancing the crosscutting reflection by the SW-based methods cannot be judged because of the limitation to only a portion of the profile length. The example presented here suggests that different methods can be complementary and that SW can be utilized to estimate P-wave weathering layer static corrections.

Acknowledgements

This study was carried out within the Smart Exploration project. Smart Exploration has received funding from the European Union's Horizon 2020 research and innovation programme under grant agreement No. 775971. Data was processed using GLOBE Claritas™ & GeoTomo (for Tomostatics).

References

Alshuhail, A., A. Aldawood, and S. Hanafy [2012]. Application of super-virtual seismic refraction interferometry to enhance first arrivals: A case study from Saudi Arabia. The Leading Edge, 31(1), p. 34–39.

Boiero, D. [2009]. Surface wave analysis for building shear wave velocity models. Ph.D. Thesis.

Boiero, D. and L. V. Socco [2014]. Joint inversion of Rayleigh-wave dispersion and P-wave refraction data for laterally varying layered models. Geophysics 79(4), EN49–EN59.

Bräunig, L., S. Buske, A. Malehmir, E. Bäckström, M. Schön, and P. Marsden [2019]. Seismic depth imaging of iron-oxide deposits and their host rocks in the Ludvika mining area of central Sweden. Geophysical Prospecting, 68(1), p. 24–43.

Eaton, D. W., B. Milkereit, and M. H. Salisbury (eds.) [2003]. Hardrock Seismic Exploration. Society of Exploration Geophysicists.

Malehmir, A. et al. [2019]. Smart Exploration: from legacy data to state-of-the- art data acquisition and imaging. First Break, 37, p. 5.

Malehmir, A., G. Maries, E. Bäckström, M. Schön, and P. Marsden [2017]. Developing cost-effective seismic mineral exploration methods using a landstreamer and a drophammer. Scientific Reports, 7(1).

Markovic, M., G. Maries, A. Malehmir, J. von Ketelhodt, E. Bäckström, M. Schön, and P. Marsden [2020]. Deep reflection seismic imaging of iron-oxide deposits in the Ludvika mining area of central Sweden. Geophysical Prospecting, 68(1), p. 7–23.

Papadopoulou, M., F. Da Col, B. Mi, E. Bäckström, P. Marsden, B. Brodic, A. Malehmir, and L. V. Socco [2020]. Surface-wave analysis for static corrections in mineral exploration: A case study from central Sweden. Geophysical Prospecting, 68(1), p. 214–231.

Place, J., and A. Malehmir [2016]. Using supervirtual first arrivals in controlled-source hardrock seismic imaging-well worth the effort. Geophysical Journal International, 206(1), p. 716–730.

Socco, L.V and C. Comina [2017]. Time-average velocity estimation through surface-wave analysis: Part 2 - P-wave velocity. Geophysics 82(3), U61–U73.

Woodward, M. J. [1992]. Wave-equation tomography. Geophysics, 57(1), p. 15–26.

Zhang, J., and M. N. Toksöz [1998]. Nonlinear refraction traveltime tomography. Geophysics, 63(5), p. 1726–1737.

Socco L.V., C. Comina and F. Khosro Anjom, [2017]. Time-average velocity estimation through surface-wave analysis: Part 1 - S-wave velocity: GEOPHYSICS, 82, 3, U49–U59.